prosthesis

MDPI

Article

Evaluation of Bone Turnover around Short Finned Implants in Atrophic Posterior Maxilla: A Finite Element Study

Andrii Kondratiev [1,2,*], Vladislav Demenko [3], Igor Linetskiy [4], Hans-Werner Weisskircher [5] and Larysa Linetska [6]

[1] Department of Materials Science and Engineering of Composite Structures, O.M. Beketov National University of Urban Economy in Kharkiv, Marshal Bazhanov Str. 17, 61002 Kharkiv, Ukraine
[2] Department of Engineering, University of Cambridge, Trumpington Str., Cambridge CB2 1PZ, UK
[3] Department of Aircraft Strength, National Aerospace University "Kharkiv Aviation Institute", Chkalova Str. 17, 61070 Kharkiv, Ukraine; v.demenko@khai.edu
[4] Department of Oral and Maxillofacial Surgery, General University Hospital in Prague, U Nemocnice 499/2, 128 08 Prague, Czech Republic; igor.linetskiy@gmail.com
[5] Private Practice, Bahnhofstrasse 7, 54298 Igel, Germany; weisskircher@t-online.de
[6] Department of Rehabilitation Medicine, National Technical University "Kharkiv Polytechnic Institute", Kyrpychova Str. 2, 61002 Kharkiv, Ukraine; larisa.linetska@gmail.com
* Correspondence: andrii.kondratiev@kname.edu.ua

Abstract: Background/Objectives: Dental implants have emerged as a modern solution for edentulous jaws, showing high success rates. However, the implant's success often hinges on the patient's bone quality and quantity, leading to higher failure rates in poor bone sites. To address this issue, short implants have become a viable alternative to traditional approaches like bone sinus lifting. Among these, Bicon® short implants with a plateau design are popular for their increased surface area, offering potential advantages over threaded implants. Despite their promise, the variability in patient-specific bone quality remains a critical factor influencing implant success and bone turnover regulated by bone strains. Excessive strains can lead to bone loss and implant failure according to Frost's "Mechanostat" theory. To better understand the implant biomechanical environment, numerical simulation (FEA) is invaluable for correlating implant and bone parameters with strain fields in adjacent bone. The goal was to establish key relationships between short implant geometry, bone quality and quantity, and strain levels in the adjacent bone of patient-dependent elasticity to mitigate the risk of implant failure by avoiding pathological strains. **Methods**: Nine Bicon Integra-CP™ implants were chosen. Using CT scans, three-dimensional models of the posterior maxilla were created in Solidworks 2022 software to represent the most challenging scenario with minimal available bone, and the implant models were positioned in the jaw with the implant apex supported by the sinus cortical bone. Outer dimensions of the maxilla segment models were determined based on a prior convergence test. Implants and abutments were considered as a single unit made of titanium alloy. The bone segments simulated types III/IV bone by different cancellous bone elasticities and by variable cortical bone elasticity moduli selected based on an experimental data range. Both implants and bone were treated as linearly elastic and isotropic materials. Boundary conditions were restraining the disto-mesial and cranial surfaces of the bone segments. The bone–implant assemblies were subjected to oblique loads, and the bone's first principal strain fields were analyzed. Maximum strain values were compared with the "minimum effective strain pathological" threshold of 3000 microstrain to assess the implant prognosis. **Results**: Physiological strains ranging from 490 to 3000 microstrain were observed in the crestal cortical bone, with no excessive strains detected at the implant neck area across different implant dimensions and cortical bone elasticity. In cancellous bone, maximum strains were observed at the first fin tip and were influenced by the implant diameter and length, as well as bone quality and cortical bone elasticity. In the spectrum of modeled bone elasticity and implant dimensions, increasing implant diameter from 4.5 to 6.0 mm resulted in a reduction in maximum strains by 34% to 52%, depending on bone type and cortical bone elasticity. Similarly, increasing implant length from 5.0 to 8.0 mm led to a reduction in maximum strains by 15% to 37%. Additionally, a two-fold reduction in cancellous bone elasticity modulus (type IV vs. III) corresponded to an increase in maximum strains by 16% to 59%. Also, maximum strains increased by 86% to 129% due

Citation: Kondratiev, A.; Demenko, V.; Linetskiy, I.; Weisskircher, H.-W.; Linetska, L. Evaluation of Bone Turnover around Short Finned Implants in Atrophic Posterior Maxilla: A Finite Element Study. *Prosthesis* **2024**, *6*, 1170–1188. https://doi.org/10.3390/prosthesis6050084

Academic Editor: Kelvin Ian Afrashtehfar

Received: 20 August 2024
Revised: 12 September 2024
Accepted: 18 September 2024
Published: 24 September 2024

to a decrease in patient-dependent cortical bone elasticity from the softest to the most rigid bone. **Conclusions**: The findings have practical implications for dental practitioners planning short finned implants in the posterior maxilla. In cases where the quality of cortical bone is uncertain and bone height is insufficient, wider 6.0 mm diameter implants should be preferred to mitigate the risk of pathological strains. Further investigations of cortical bone architecture and elasticity in the posterior maxilla are recommended to develop comprehensive clinical recommendations considering bone volume and quality limitations. Such research can potentially enable the placement of narrower implants in cases of insufficient bone.

Keywords: Frost's "mechanostat" theory; plateau implant; bone quality; FEA

1. Introduction

The success of dental implants relies on maintaining a stable attachment to the bone tissue, which is influenced by various factors including bone availability and quality, implant design, and dimensions. Effective remodeling of the bone is essential for supporting secure anchoring, with bone restructuring being particularly important [1,2].

Although dental implant treatments often have high success rates, long-term success can be challenged by different biomechanical factors [3]. The posterior maxillary region, in particular, is at greater risk of failure due to insufficient bone density, reduced bone volume, and increased masticatory forces, indicating poor bone quality [4,5].

Short implants have emerged as a practical solution in compromised conditions, especially in the maxillary molar region, eliminating the need for bone grafting and traditional implant placement [6–8]. Studies suggest that short implants can achieve comparable success rates to longer ones [9,10]. However, their smaller surface area can lead to increased stress and strain concentrations in the crestal bone compared to conventional implants [11,12]. To mitigate this issue, the use of wide short implants has been proposed in cases of insufficient bone height and significantly higher occlusal loads in molar sites. This approach aims to increase surface area, thereby improving stress and strain distribution in the adjacent bone, particularly at the critical area of the bone–implant interface.

Plateau implants, introduced in 1985, stand out as a unique type of dental implant characterized by multiple parallel circular threads known as plateau or fins. Among these, the Bicon® screwless design, featuring a plateau root-formed body, is widely utilized [13,14]. Notably, it provides 30% more surface area compared to threaded implants of similar size. These implants are especially recommended for patients with inadequate bone height, and their short lengths (<8 mm) help eliminate the need for preoperative procedures like grafting or sinus lifting. The increased surface area of bone–implant contact in plateau implants reduces stresses and strains by enhancing load transfer along the bone–implant interface, which is particularly advantageous when bone height is limited.

Plateau implants demonstrate significant efficacy in preventing bone loss, facilitated by the creation of 'healing chambers'—hollow spaces between the implant and bone. These chambers, formed due to the interaction between implant design and drilling dimensions, promote the development of intramembranous-like woven bone formation [14–16]. These spaces are initially filled by the blood clot immediately after implantation and gradually filled by new bone apposition over time.

Numerous studies have investigated the behavior of short implants, examining factors such as diameter, length, and macrostructure, as well as the bone healing response to different implant root shapes and the cumulative survival rates of short implants. The refinement of plateau root form designs has significantly increased the cumulative survival rate to over 90%, optimizing biological responses during early endosseous peri-implant healing.

Successful osseointegration of the implant with marginal bone significantly increases the implant's load-bearing capacity and bone turnover regulation. However, predicting the mechanical behavior of the bone–implant interface remains challenging due to variations

in patient-specific cortical bone elasticity and strength. Bone strains are recognized as mechanical stimuli that influence bone turnover and maintain mechanical strength through primary cilia in bone-forming cells [16,17]. This process ensures the adaptation of bone morphology to functional loads throughout an individual's life. Biomechanical feedback, in line with Frost's "bone mechanostat" hypothesis, regulates the relationship between bone density and load magnitude, optimizing bone structure through modeling and remodeling. According to Frost, when bone strains surpass the "minimum effective strain pathological" threshold (MESp = 3000 microstrain), microdamages accumulate, leading to bone failure [18]. To promote peri-implant bone mass, strains should be maintained above the minimum effective strain modeling threshold (MESm) of 1000–1500 microstrain [19,20].

Predicting treatment success and the longevity of implants hinges on selecting dimensions that align with a safe strain spectrum and the available bone quantity. This process typically involves an initial evaluation of the patient's jaw bone properties, taking into account factors like placement site, bone shape, and dimensions. However, it often overlooks the physical and mechanical properties of bone tissues, which are crucial for preventing bone resorption. In cases of thin, atrophic bone where the cancellous bone core lacks reliability as a load-bearing element, understanding the impact of adjacent bone elasticity on neck area strains becomes paramount. Selecting suitable implants becomes particularly challenging when dealing with poor bone quality, insufficient volume, and variations in cortical bone mechanical properties [21].

To address the complex issue of correlating implant geometry and dimensions with bone properties and strains, computer modeling, specifically, finite element analysis (FEA), proves invaluable [4,22]. FEA allows for the assessment of strain concentrations in peri-implant bone, considering factors such as implant shape, dimensions, bone quality, and quantity [23]. This approach provides a comprehensive understanding of implant biomechanics under functional loads, aiding in the selection of appropriate implants for each unique patient scenario [24].

Several studies have explored finite element (FE) strain analysis in adjacent bone, examining the biomechanical effects of implant dimensions and bone quality in osseointegrated and immediate implants [22,23,25]. However, these studies present a wide range of strain magnitudes that do not directly correlate with the pathological strain threshold at the critical area of the bone–implant interface, where maximal strains may trigger bone loss. As a result, these findings cannot reliably predict implant success or failure or provide recommendations for implant sizing selection, especially in compromised maxillary cases.

The objective of this study was to use FEA simulation to evaluate the impact of short finned implants and crestal bone quality/quantity on strain magnitudes in adjacent cortical bone with patient-variable elasticity. The aim was to characterize bone turnover in the posterior maxilla and recommend the placement of Bicon Integra-CP™ short plateau implants based on their post-osseointegration perspective. This assessment sought to ensure their ability to withstand functional loading and prevent cortical bone loss.

2. Materials and Methods

Nine different geometric designs of Bicon Integra-CP™ implants (Bicon, Boston, MA, USA) were investigated, varying in length (5.0 mm for S, 6.0 mm for I, and 8.0 mm for L) and diameter (4.5 mm for N, 5.0 mm for M, and 6.0 mm for W). To model these implants and abutments, their dimensions and designs were obtained using digital calipers, photographs, and images captured with a light optic microscope.

To create solid models of posterior maxilla alveolar bone segments, computed tomographic (CT) images from unidentified patients were selected from the authors' CT database to delineate cortical and cancellous bone contours. Simplified 3D geometry segments with a length of 40 mm were reconstructed using these CT images in DICOM format with Solidworks 2022 software (Dassault Systemes SolidWorks Corporation, Waltham, MA, USA).

The 3D models of the implants were crestally placed into nine posterior maxilla segment models including 0.5 mm of crestal cortical bone. They represented type III/IV bone (classified according to Lekholm and Zarb) simulated by varying the cancellous bone modulus of elasticity (1.37/0.69 GPa) (see Figure 1).

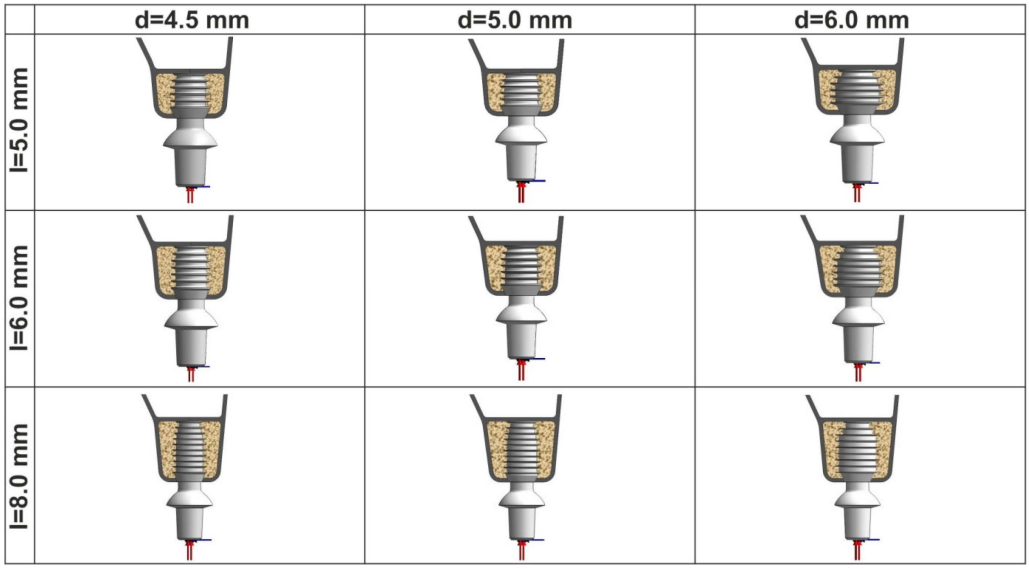

Figure 1. Maxillary bone segments with nine inserted implants. Oblique loading is applied to the center of abutment upper surface at 7.0 mm distance from the upper bone margin.

The size of the maxilla segment model was 40 × 13 × 9 mm (length × height × width), determined based on a previous convergence test. The dimensions were chosen to replicate the most critical scenario of minimal available bone, necessitating crestal placement as a necessary compromise.

Implant and bone tissues were considered to be linearly elastic and isotropic, with homogeneous material volumes. Implants and abutments were treated as a continuous unit and were assumed to be made of titanium alloy, with a modulus of elasticity of 114 GPa and a Poisson's ratio of 0.34 [26]. The Poisson's ratio for both cortical and cancellous bone tissues was assumed to be 0.3 [27].

For computer simulation, a spectrum of elasticity moduli representing different levels of human cortical bone elasticity was selected based on experimental investigations, ranging from 4.0 to 13.7 GPa [21]. The elasticity moduli were assigned as follows: E_1 = 13.7 GPa, E_2 = 12.0 GPa, E_3 = 10.0 GPa, E_4 = 8.0 GPa, E_5 = 6.0 GPa, and E_6 = 4.0 GPa.

The boundary conditions involved restraining the disto-mesial surfaces of the bone segment as well as the cranial surfaces in all models (see Figure 2). Functional loading of the implant was simulated at the center of a 7 Series Low 0° abutment in three dimensions. A mean maximal functional load of 120.9 N was applied obliquely at an angle of approximately 75° to the abutment top surface [28]. The loading components were determined as 116.3 N in the axial direction, 17.4 N lingually, and 23.8 N disto-mesially. The last two components represented the resultant vector of a 29.5 N horizontal functional load acting in the plane of the critical bone–implant interface [24,28,29]. The implants were assumed to be fully osseointegrated [30].

A numerical analysis of bone–implant models was conducted using FE software Solidworks Simulation (Dassault Systemes SolidWorks Corporation, Waltham, MA, USA). A mesh convergence analysis was performed to determine the optimal element size.

The mesh refinement process involved gradually reducing the element sizing from 2.0 mm to 0.010 mm, and the change in the maximum first principal strain in the bone–implant interface was studied. The maximum strain converged toward a finite value as the mesh density increased, with a convergence criterion set to less than 2% for the changes in

the maximal strain of all the elements [31,32]. The analysis was stopped at the FEA size of 0.020 mm. The total number of 3D finite elements ranged from 1,659,134 to 2,000,652, and the nodes ranged from 2,238,052 to 2,695,410. An example of FE meshing for a 5.0 × 5.0 mm implant is provided in Figure 3.

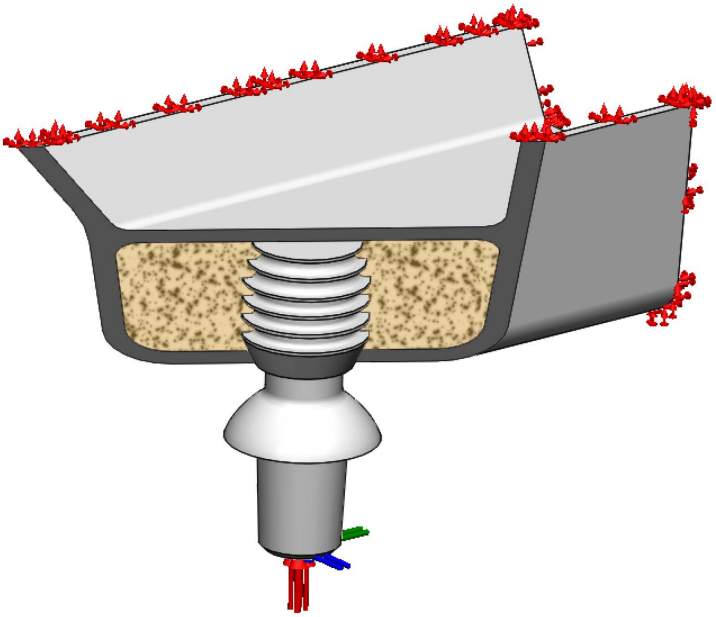

Figure 2. Illustration of 3D view of 5.0 × 5.0 mm implant placed in maxillary bone segment with 0.5 mm crestal and sinus cortical bone thickness. Oblique loading is applied at the center of 7 Series Low 0° abutment upper surface at 7.0 mm distance from the upper bone margin. Disto-mesial and cranial surfaces of the bone segment are restrained.

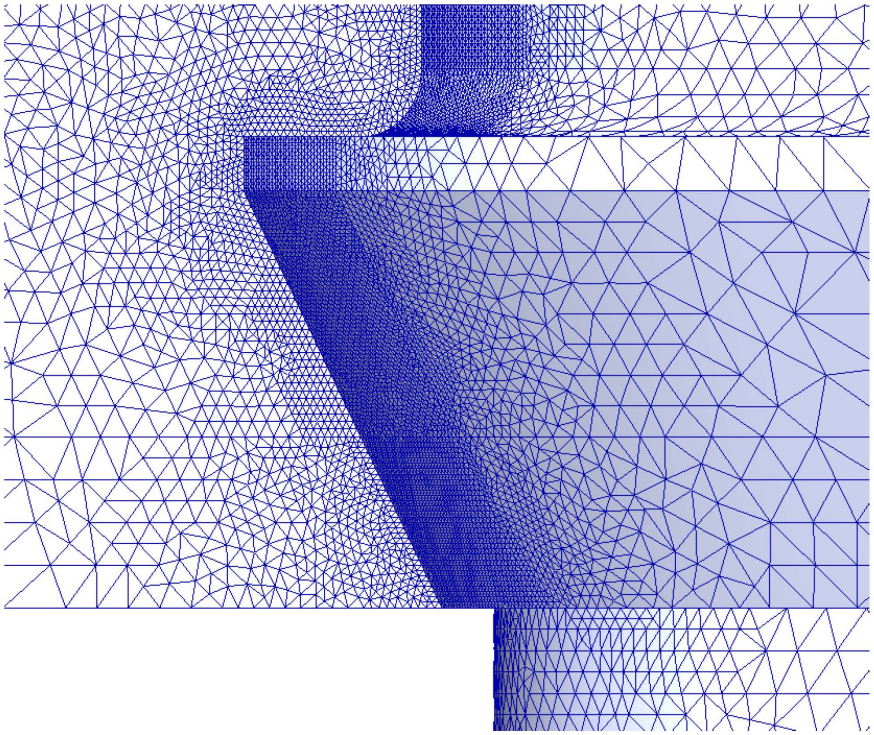

Figure 3. FE meshing of maxillary bone segment with 0.5 mm crestal and sinus cortical bone and 5.0 × 6.0 mm implant with mapped meshing in the neck area of bone–implant interface. Minimal FE size is 0.020 mm.

In the bone–implant assembly strain analysis, first principal strains (FPSs) were chosen as the measure of bone turnover. FPS localizations in the peri-implant area of the critical bone–implant interface were studied for 108 bone–implant combinations (9 bone–implant models × 2 bone types × 6 cortical bone elasticity moduli) to determine maximal FPS (MFPS). These values were then correlated with 3000 microstrain threshold (MFPSp) to evaluate implant lifetime prognosis in terms of physiological/pathological bone strains in the anchorage area [18–20].

3. Results

The distributions of FPS at the bone–implant interface is depicted in Figure 4, while Figure 5 displays the variation of FPS along the critical bone–implant contact length.

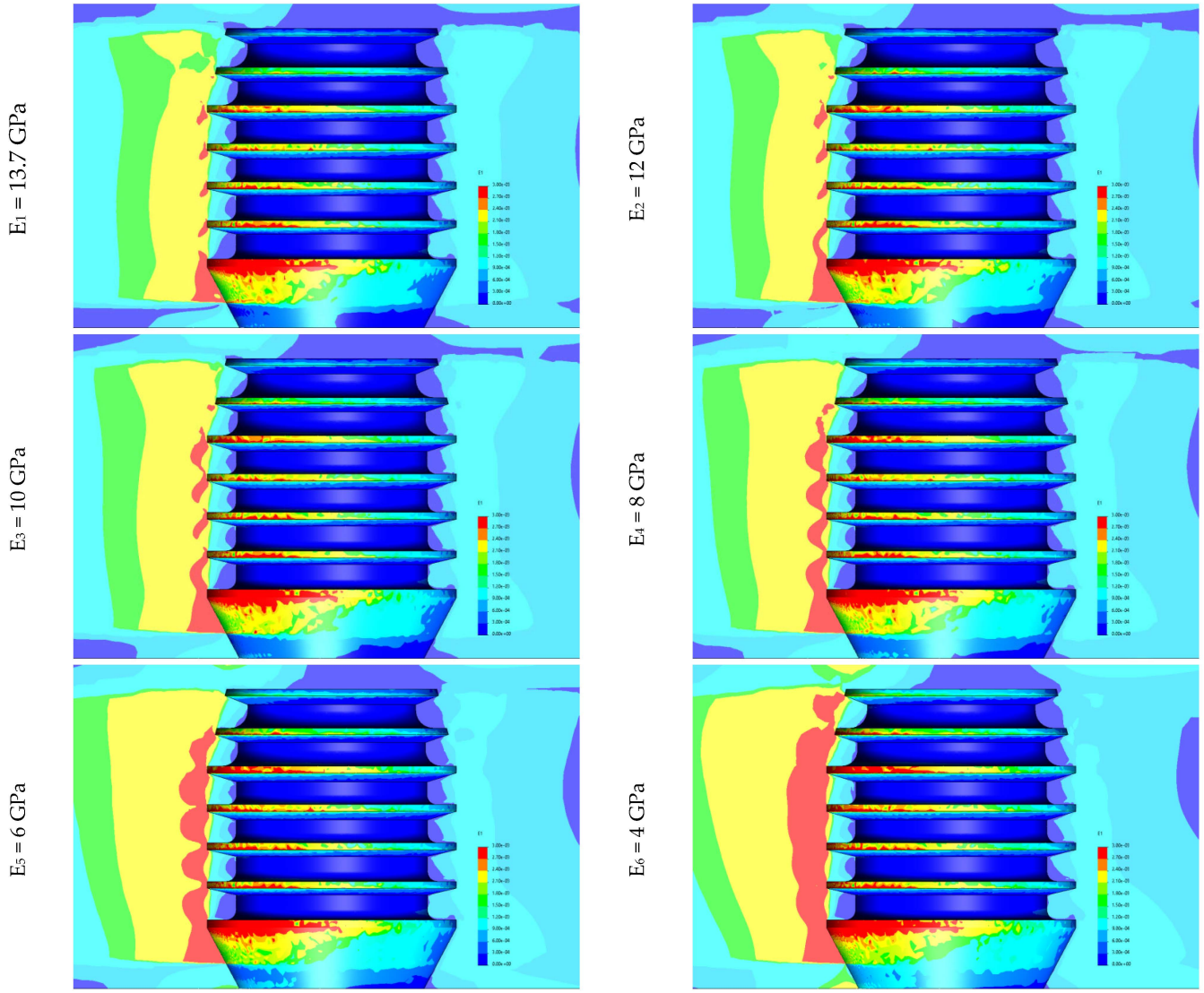

Figure 4. First principal strain localization in the plane of the critical bone–implant interface for the studied 5.0 × 6.0 mm Bicon SHORT® implant, type IV bone, and six degrees of cortical bone elasticity corresponding to E_1–E_6 moduli of elasticity.

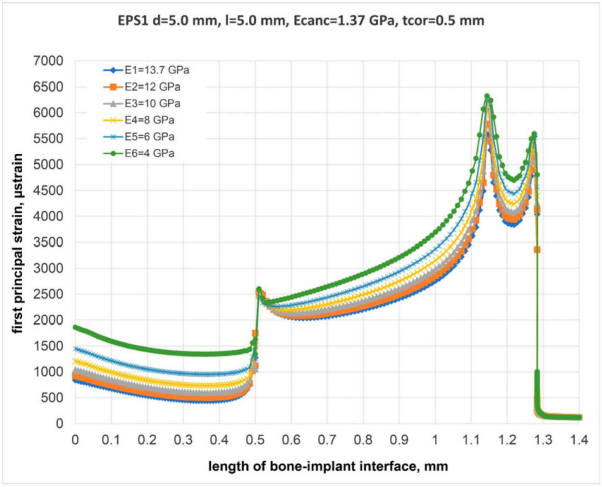

top left

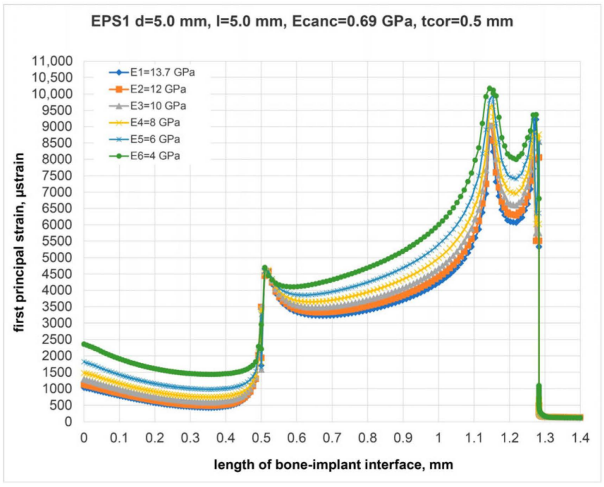

top right

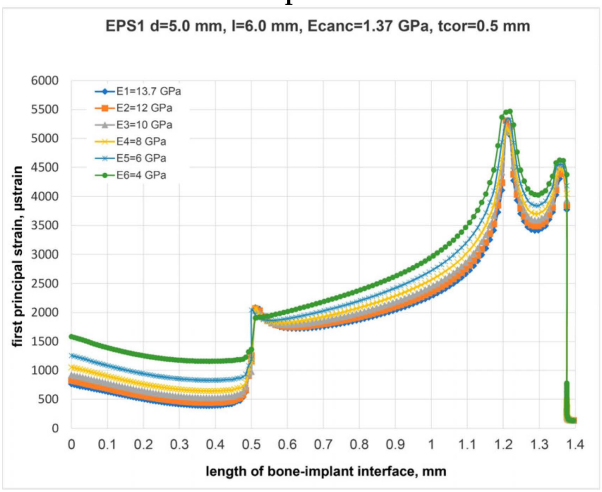

middle left

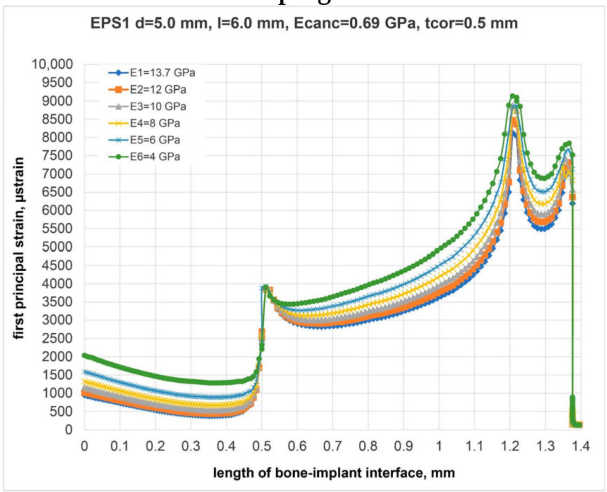

middle right

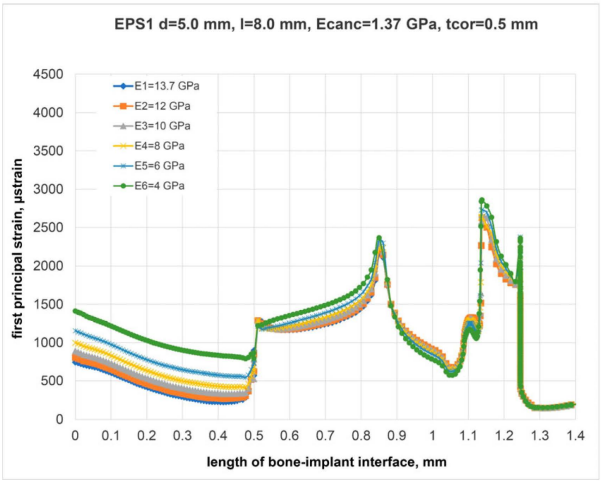

bottom left

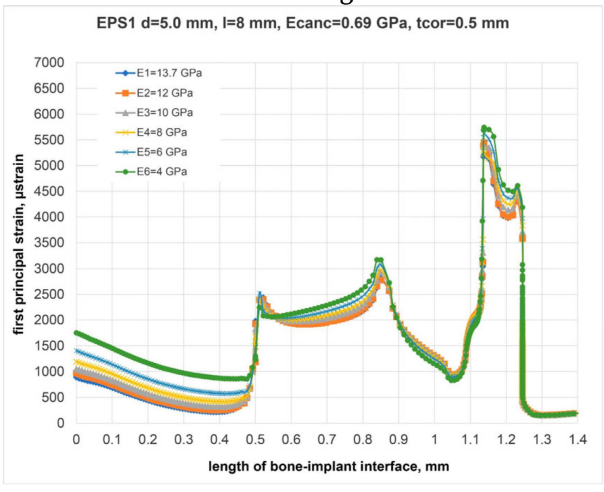

bottom right

Figure 5. Illustration of first principal strain distribution along the critical line of bone–implant interface for 5.0 × 5.0 mm (**top**), 5.0 × 6.0 mm (**middle**), 5.0 × 8.0 mm (**bottom**) implants placed into bone segments of types III (**left**) and IV (**right**) bone (E_{III} = 1.37 GPa and E_{IV} = 0.69 GPa) at E_1–E_6 degrees of cortical bone elasticity.

Maximal magnitudes of FPS (MFPSs) were sought, particularly on the surface of cortical bone, influenced by factors such as implant dimensions, cortical bone elasticity, and bone quality (Figures 4–7).

The analysis revealed that there were no instances of overstrains (MFPS > 3000 µstrain) at the implant neck area. Instead, a spectrum of safe maximal MFPS (490–3000 µstrain) was observed in the crestal cortical bone, with W implants causing strains ranging from 490 to 1860 µstrain and N implants inducing strains from 860 to 3000 µstrain. In cancellous bone, MFPSs were located at the first fin position, similarly influenced by implant dimensions, bone quality, and cortical bone elasticity.

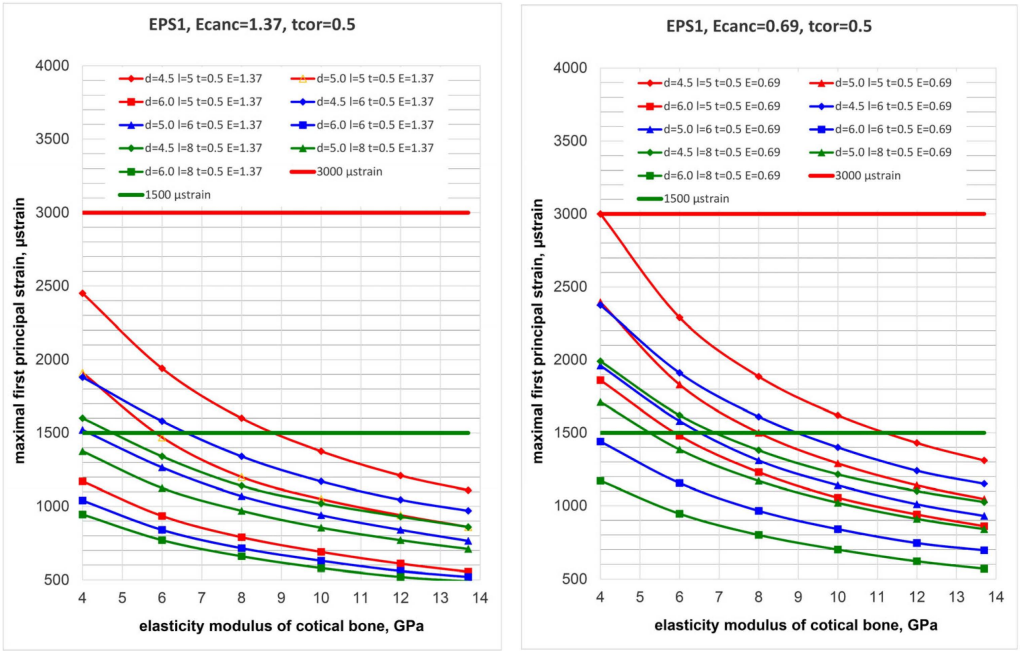

Figure 6. Dependence of maximal first principal strains (MFPSs) in cortical bone on its modulus of elasticity for the spectrum of implants placed into bone segments with 0.5 mm cortical bone thickness for type III (**left**) and IV (**right**) bone and the studied degrees of patient-specific cortical bone elasticity E_1–E_6. Red line corresponds to 3000 microstrain of Frost "minimum effective strain pathological" (MESp).

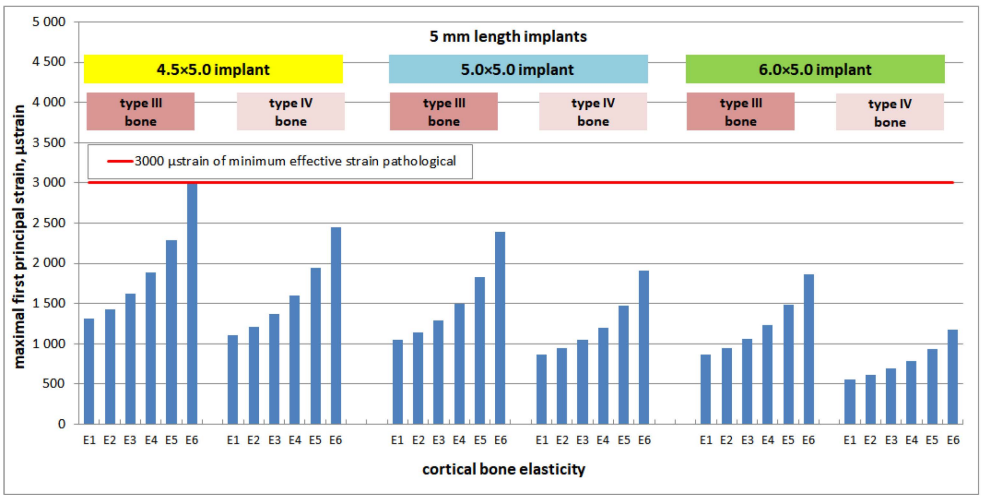

top

Figure 7. *Cont.*

Figure 7. Dependence of maximal first principal strains (MFPSs) in cortical bone on its modulus of elasticity for implants of length 5.0 mm (**top**), 6.0 mm (**middle**), 8.0 mm (**bottom**) placed into bone segments of type III and IV bone and the studied E1–E6 degrees of patient-specific cortical bone elasticity. Red line corresponds to 3000 microstrain of Frost "minimum effective strain pathological" (MESP).

For a range of cortical bone elasticity (E_1–E_6) and type III bone, increasing implant diameter from 4.5 to 6.0 mm resulted in FPS reductions of approximately 50% for S-implants, 47% for I-implants, and 43% for L-implants. In type IV bone under similar conditions, FPS reductions were around 36%, 40%, and 42% for S-, I-, and L-implants, respectively. These trends are depicted in Figures 8 and 9.

For the E1–E6 spectrum of cortical bone elasticity and type III bone, MFPS reduction due to increase in length from 5.0 to 8.0 mm was (23–35) % for N-implants, (17–28)% for M-implants, and (12–19) % for W-implants. For type IV bone and otherwise same conditions, the corresponding FPS reduction was (22–34) % for N-implants, (20–29) % for M-implants, and (34–37) % for W-implants. These findings are illustrated in Figures 10 and 11.

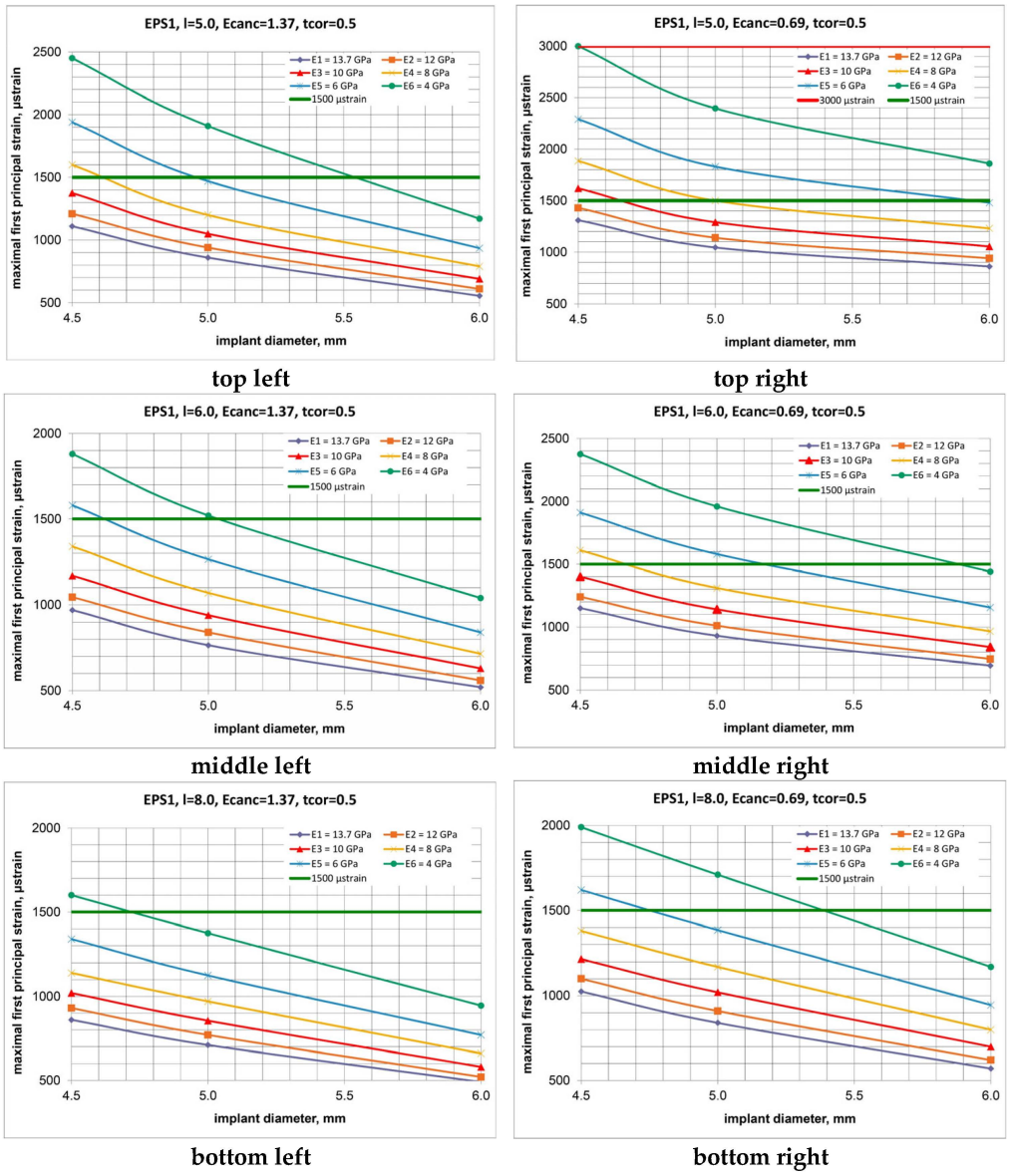

Figure 8. Maximal first principal strains' (MFPSs') dependence on the implants' diameter increase for implants of length 5.0 mm (**top**), 6.0 mm (**middle**), 8.0 mm (**bottom**) placed into bone segments of type III (**left**) and IV (**right**) bone and the studied E_1–E_6 degrees of patient-specific cortical bone elasticity. Red line corresponds to 3000 microstrain of Frost "minimum effective strain pathological" (MESP).

Bone quality was found to have a substantial impact on the biomechanical state of cortical bone: for N, M, and W implants, a two-fold reduction in elasticity modulus (0.69 against 1.37 GPa) corresponded to an 18, 22, and 55% MFPS rise for S-implants, 19, 22, and 34% MFPS rise for I-implants, and 19, 18, and 16% MFPS rise for L-implants. These data correspond to the E1 level of cortical bone elasticity. For the E2, E3, E4, E5, and E6 levels, the corresponding MFPS rise was as follows: E2 level—18, 21, and 54% (S-implants), 19, 20, and 33% (I-implants), and 19, 19, and 21% (L-implants); E3 level—18, 23, and 53% (S-implants), 20, 21, and 33% (I-implants), and 19, 19, and 21% (L-implants); E4 level—18, 25, and 56% (S-implants), 20, 22, and 35% (I-implants), and 21, 21, and 22% (L-implants)); E5 level—18, 24, and 58% (S-implants), 21, 25, and 38% (I-implants), and 21, 22, and 23% (L-implants)); E6 level—22, 25, and 59% (S-implants), 26, 29, and 38% (I-implants), and 24, 24, and 25% (L-implants). The percentage of MFPS rise is illustrated in Figure 12.

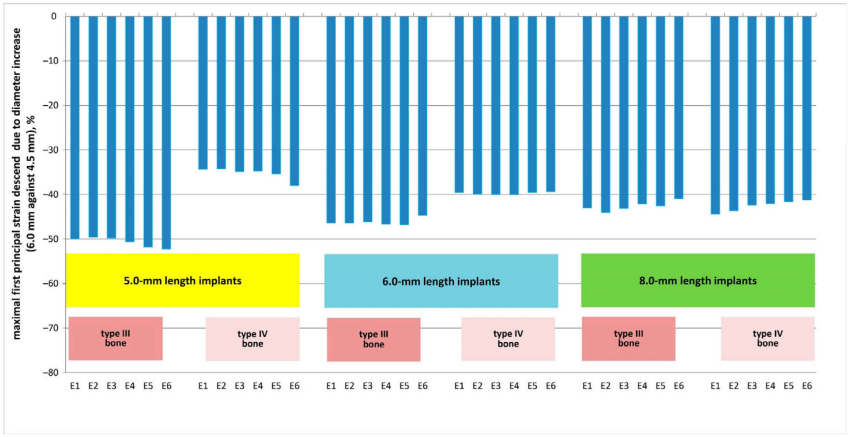

Figure 9. Maximal first principal strain (MFPS) reduction due to the implants' diameter increase from 4.5 mm to 6.0 mm for the spectrum of implants placed into bone segments of types III and IV bone.

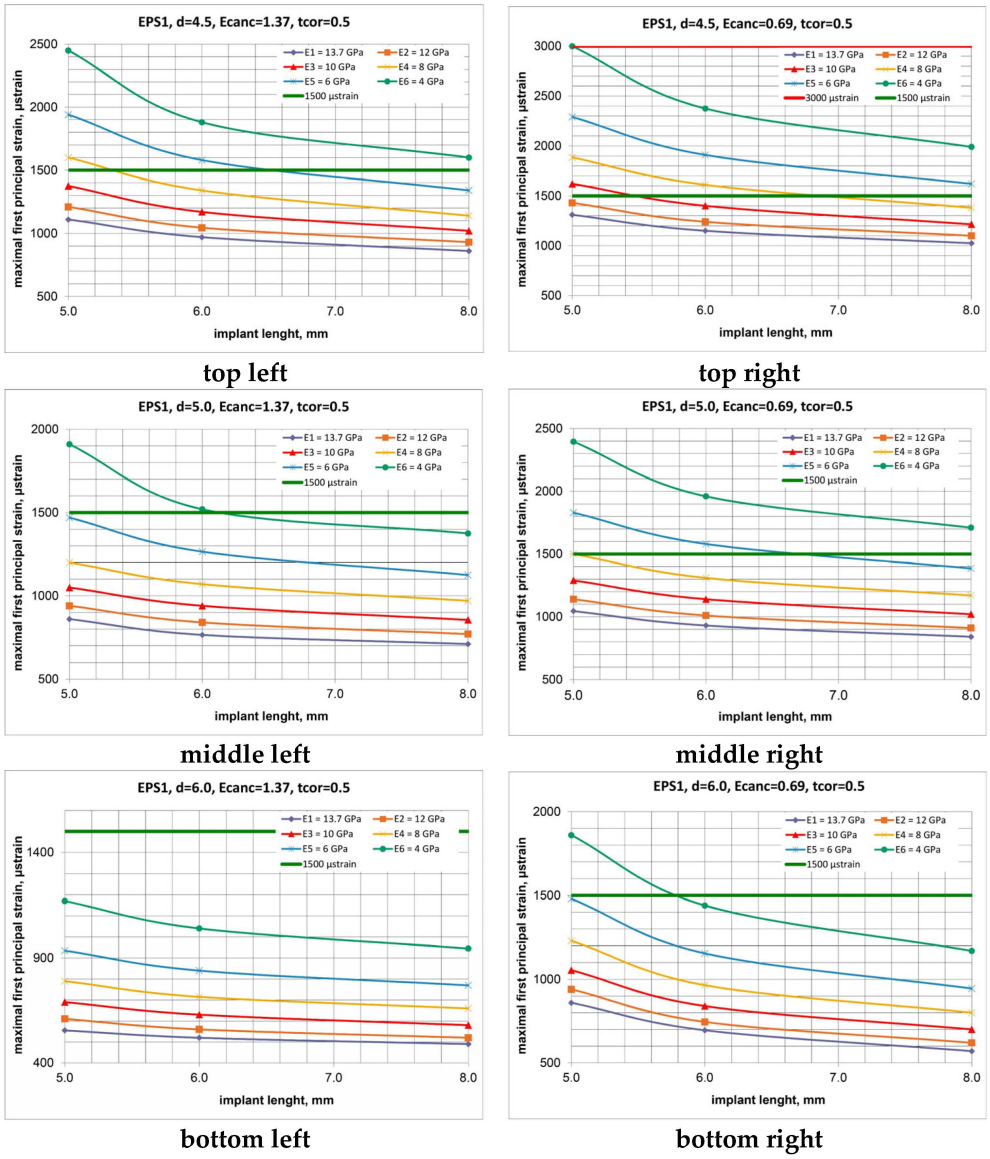

Figure 10. Maximal first principal strain (MFPS) dependence on the implants' length increase for implants of diameter 4.5 mm (**top**), 5.0 mm (**middle**), 6.0 mm (**bottom**) placed into bone segments of

type III (**left**) and IV (**right**) bone and the studied E_1–E_6 degrees of patient-specific cortical bone elasticity. Red line corresponds to 3000 microstrain of Frost "minimum effective strain pathological" (MESp).

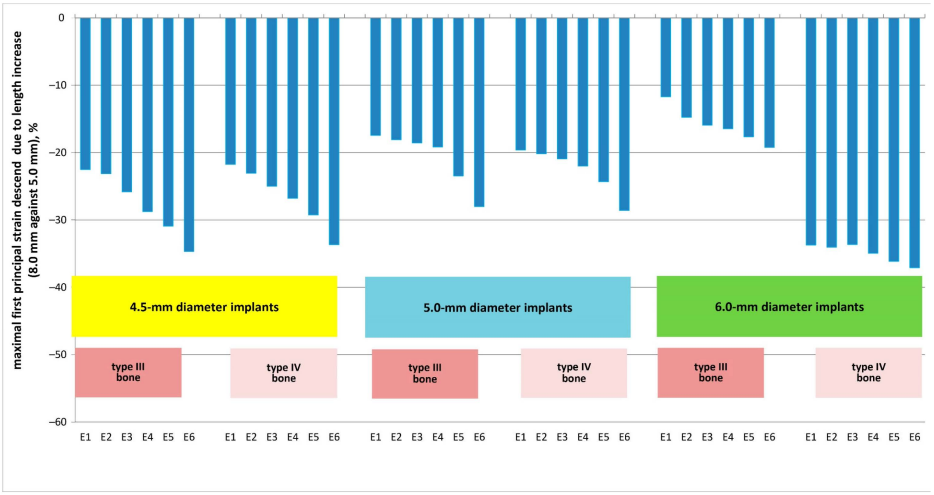

Figure 11. Maximal first principal strain (MFPS) reduction due to the implants' length increase from 4.5 mm to 6.0 mm for the spectrum of implants placed into bone segments of types III and IV bone.

A reduction in cortical bone elasticity caused its significant overstrain: for N-, M-, W-implants, the MFPS rise due to decrease in cortical bone rigidity (E6 against E1) for type III bone was 121/122/111, 94/99/101, and 86/94/93% (S-/I-/L-implants). For type IV bone, cortical bone and implant parameters, the MFPS rise was 129/129/116, 107/110/107, and 94/104/105% (S-/I-/L-implants). The results of an MFPS rise (percentage) are illustrated in Figure 13.

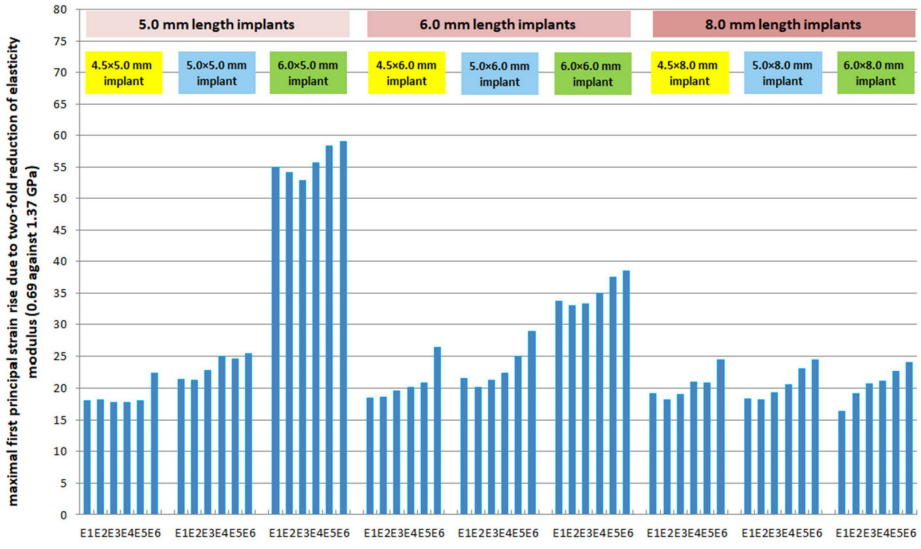

Figure 12. Impact of bone quality on maximal first principal strain (MFPS) rise in terms of two-fold reduction in the cancellous bone elasticity modulus (0.69 against 1.37 GPa) for the spectrum of implants placed into bone segments at E_1–E_6 degrees of cortical bone elasticity.

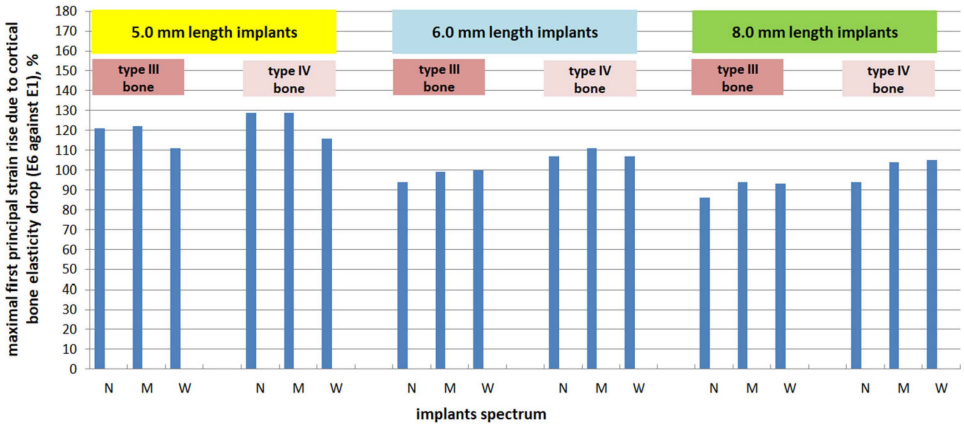

Figure 13. Maximal first principal strain (MFPS) rise due to cortical bone elasticity reduction (E_6 against E_1).

4. Discussion

Studying the strain fields induced by osseointegrated implants of varying sizes in the anchorage area of the maxilla, often characterized by insufficient volume and low quality (types III and IV), is crucial for achieving optimal transfer of functional loads to marginal bone and ensuring physiological turnover. In compromised conditions like these, understanding the impact of cortical bone elasticity on neck area strains becomes a priority, particularly in terms of bone turnover. However, relying solely on clinical and experimental studies may not fully address the biomechanical response, especially considering patient-variable bone elasticity on loading transfer. Establishing quantitative relationships between key influencing parameters such as mechanical stresses and strains in bone, maxillofacial system geometry and dimensions, material properties, and bone quality, and subsequently selecting patient-personified implants, requires advanced methods of analysis.

Computer modeling serves as a contemporary in silico approach to comprehending the biomechanical behavior of implants and implant-supported restorations, as well as predicting implant lifetime by maintaining tolerable strain concentrations in peri-implant bone to facilitate adequate bone turnover through viable implant selection [22,23,25,33–37].

Although several finite element (FE) studies have analyzed strain distribution in adjacent bone concerning implant dimensions and bone quality [25,35,38], their findings primarily help in refining the parameters of a bone–implant system rather than assessing the risk of structural failure. While some studies have considered strains in evaluating bone's mechanical behavior, they have struggled to establish clear patterns linking specific implant dimensions, adjacent bone quality, and the origins of pathological bone strains (see, for example, [16]).

The issues outlined above underscore the objective of this study, wherein we aimed to establish a methodological framework for selecting viable implants based on finite element analysis and Frost's "Mechanostat" theory. This method enables the prediction of safe strains in adjacent bone by appropriately sizing the implant, considering the quality and quantity of patient-specific bone. This approach appears more effective than the conventional clinical procedure, which typically involves a preliminary examination of the patient's jaw bone properties, such as placement site, bone shape, and dimensions. However, this conventional method overlooks the physical and mechanical properties of bone tissues, which are crucial indicators of potential bone failure.

Therefore, the proposed method offers an advantage in addressing the clinically significant issue of implant selection, as it theoretically predicts the success of implant treatment by preventing pathological bone strains. This methodology allows for the identification of specific requirements regarding both the quality/rigidity of the bone and the size of the implant necessary for successful placement in a particular patient's

bone. Consequently, this lays the groundwork for the development of tailored clinical recommendations for implant selection.

Despite the abundance of finite element analysis (FEA) studies on bone–implant interaction over the past five decades, the reliability and precision of these in silico investigations are not always beyond dispute. It has been emphasized [39] that FEA studies of biological structures should ideally undergo experimental validation whenever feasible. Additionally, it has been suggested [40] that FEA studies should meet minimum requirements, including comparisons with data from other studies or real-world observations. According to the American Society of Mechanical Engineers Committee on verification and validation in computational solid mechanics, verification is defined as "the process of determining that a computational model accurately represents the underlying mathematical model and its solution", while validation is defined as "the process of determining the degree to which a model is an accurate representation of the real world from the perspective of the intended uses of the model". In simple terms, verification is the process of "solving the equations right", whereas validation is the process of "solving the right equations" [41]. Given these contentious circumstances, our focus was on ensuring the high accuracy of our computations. We conducted an adequate mesh convergence test to determine the optimal element size, thus enhancing the reliability of our results.

Despite the high precision of finite element (FE) analysis, its limitations stem from the assumptions and simplifications adopted, which directly affect the accuracy of strain calculations. One major limitation is the design of an adequate 3D bone segment model. On one hand, it is necessary to eliminate the effects of patient-specific anatomical variations to ensure the comparability of results across different models [42]. On the other hand, the difference between the actual anatomic models of maxilla and the 3D computer model should be minimal [43]. To strike a balance, we first developed 3D models of the maxilla surrounding Bicon plateau implants by importing CT images to simulate the shape and dimensions of bone components. Then, minor simplifications were made to create models that are more comparable and universally applicable in a biomechanical context, consistent with similar studies in the field [35,42,44,45].

In most studies examining the biomechanical behavior of dental implant systems, the implant is assumed to be 100% osseointegrated [22,30,35,43,44], with no sliding allowed between the implant and the bone. In reality, osseointegration does not occur clinically [30,46]. It is highly dependent on bone quality, healing process, and loads applied to the implant during function [4]. Therefore, deviating from the concept of complete osseointegration in the present comparative study would have introduced significant uncertainties into the results, making it impossible to compare them with those of other authors. Hence, the concept of complete osseointegration was incorporated into the designed algorithm of numerical analysis.

In our designed models, all structures were assumed to be homogeneous, isotropic, and linearly elastic, consistent with many contemporary studies in the field [35,44]. However, clinical reality and material properties differ from these assumptions. Cortical bone, for example, is transversely isotropic and inhomogeneous; bone anisotropy better reflects actual clinical conditions [46,47], and it is more appropriate in simulating actual clinical conditions. Undoubtedly, detailed architecture and morphology of each bone layer, if included in the model, may provide more realistic strain fields and could result in significant local variations in bone strains. While including detailed architecture and morphology of each bone layer in the model could provide more realistic strain fields and lead to significant local variations in bone strains, studies such as Limbert et al.'s micro-CT-based work [48] have shown that bone strain levels remain within the homeostatic range even when these variations, partly caused by the trabecular nature of bone, are modeled in detail.

It is worth noting that Frost's experimental work also does not differentiate for these effects but provides a general guideline for bone remodeling [18,49]. Considering the challenges in obtaining adequate anisotropic elastic data and the comparative nature of our study, we opted for the widely accepted isotropic approach. Like many well-recognized

studies in the field [35,37,44], our investigation aimed to assess the biomechanical conditions of peri-implant bone behavior. However, it is important to acknowledge that future finite element models should address these issues, and bone should be analyzed as anisotropic and nonhomogeneous when more sophisticated approaches are planned to analyze living tissue behavior under mechanical loading.

To predict potential bone failure and enhance our understanding of the impact of bone quality and implant dimensions on lifetime prognosis, information on elasticity modulus is crucial. This parameter plays a fundamental role in assigning bone material properties to finite element (FE) meshes during model generation and subsequent strain analysis. While calculating heterogeneous elasticity modulus magnitudes from Digital Imaging and Communications in Medicine (DICOM) files, containing comprehensive tissue structure data, would be more appropriate, this capability is currently not widely available to most clinicians [50]. Therefore, in our study, we opted for an averaged phenomenological approach based on experimental tests of bone specimens using ultrasonic transmission techniques or nanoindentation [21]. This approach involves equalizing data across cortical and cancellous bone volumes and allows for correlation with similar research in the field, facilitating the generalization of relationships across a wide spectrum of human bone elasticity modulus variations.

In our study, we improved critical strain calculation by determining the plane of the critical bone–implant interface based on a preliminary evaluation of strain field contours. This detail enabled us to assess implant success by comparing maximal principal strain values with Frost's MESp threshold for each bone–implant system studied. This approach seemed more appropriate compared to the study [16], where "overstrain fractions" are analyzed instead of exact strain data.

Our study focuses solely on static loadings because their duration of application is brief, classifying them as static forces according to the generally accepted classification in the mechanics of deformable solids [39]. This approach aligns with most finite element studies, where static loads simulate not only vertical loads and horizontal forces but also combined loads (e.g., oblique occlusal forces) to reflect more realistic conditions and obtain a more accurate mechanical response.

Although dental implants are subjected to both static and repeated (cyclic) loads [22,44,45,51], our study does not address cyclic loading. In fact, dental implants are subjected not only to static loads but also to repeated (cyclic) loads [52]. It has been suggested that bone strength decreases when subjected to cyclic loading, potentially leading to different stress/strain calculations [53]. However, this aspect falls beyond the scope of our present study.

Despite controversial limitations, the results obtained in terms of critical stress–strain state location are in agreement with foregoing studies, in which the authors try to understand the biomechanical behavior of implants in living surroundings [25,33–36]. Same as in our study, the works mentioned above have the limitations of being a finite element simulation. Similar to their content, we have considered specific situations, like a simplified 3D bone model, standardized bone elasticity and variable quality, average cortical bone thicknesses, non-axial static loading, completely osseointegrated implants, ranked bone elasticity moduli, that do not exactly reflect clinical situations. Thus, the values obtained may not correspond to the clinical behavior of considered implant systems. It is necessary to contrast these results with those obtained in in vitro and in vivo studies where possible.

The significance of our study lies in our attempt to enhance the understanding of the fundamental processes involved in load transmission to both bone and implants and to evaluate the conditions leading to eventual failure due to pathological turnover. Additionally, we aimed to explore the relationships between principal biomechanical parameters of bone structures and dental system geometry. While our research currently offers modest clinical recommendations, future systematic studies on the ordered testing of the elastic and strength properties of cortical and cancellous bone could pave the way for establishing more robust relationships between the aforementioned parameters and the properties of the studied structures. This, in turn, will likely reduce clinical discrepancies between the results

of computer modeling and real clinical practice, reinforcing the significance of following clinical recommendations for practitioners.

5. Conclusions

According to Frost's "Mechanostat" theory, strains exceeding MESp (3000 μstrain) will cause bone failure. In order to produce a peri-implant bone mass increase after the healing period and avoid bone mass loss, strains should be kept above the MESm threshold (1000–1500 μstrain). In the present study, Frost's "Mechanostat" hypothesis was applied to establish basic relationships between the factors which predetermine implant success in terms of physiological/pathological bone turnover.

The studied implants were found to be sensitive to the spectrum of the influence factors, but the analysis revealed that there were no instances of overstrains (MFPS > 3000 μstrain) at the implant neck area of Bicon Integra-CP™ implants.

The largest effect of implant diameter increase on strain reduction in the type III bone was found for short implants for all studied levels of cortical bone elasticity and the smallest for long implants. In Type IV bone, such an effect was nondependent on the implant length.

The effect of increase in implant length on strain reduction was significantly dependent on bone quality in the case of wide implants where type IV bone provided two times more effect of strain reduction than type III bone.

A wide implant was the most sensitive to the deterioration of bone quality. It induced the most rise of bone strains than N and M implants. This trend occurred at all studied cortical bone elasticity levels, especially for most soft bone.

A significant variation of the cortical bone elasticity induced the most significant increase in cortical bone strains for all implants and bone types. The larger strain increase corresponded to narrow implants in both bone types.

The findings are useful for dental practitioners planning short finned implants in the posterior maxilla. In cases of uncertain cortical bone quality and insufficient bone height, wider implants from the Bicon Integra-CP™ catalogue should be preferred to mitigate the risk of pathological strains. Further investigations of cortical bone architecture and elasticity in the posterior maxilla site are recommended to develop comprehensive clinical recommendations considering bone volume and quality limitations. Such research can potentially enable the placement of narrower implants in cases of insufficient bone.

Author Contributions: Conceptualization, H.-W.W. and V.D.; methodology, A.K.; validation, I.L., L.L. and H.-W.W.; formal analysis, H.-W.W. and A.K.; investigation, I.L. and V.D.; resources, V.D. and L.L.; data curation, V.D., I.L. and A.K.; writing—original draft preparation, V.D. and A.K.; writing—review and editing, L.L. and H.-W.W.; visualization, H.-W.W.; supervision, A.K.; project administration, H.-W.W. and V.D. All authors have read and agreed to the published version of the manuscript.

Funding: This research received no external funding.

Institutional Review Board Statement: Not applicable.

Informed Consent Statement: Not applicable.

Data Availability Statement: The original contributions presented in the study are included in the article, further inquiries can be directed to the corresponding author.

Acknowledgments: The authors thank the University of Cambridge for their support.

Conflicts of Interest: The authors declare no conflicts of interest.

References

1. Overmann, A.L.; Aparicio, C.; Richards, J.T.; Mutreja, I.; Fischer, N.G.; Wade, S.M.; Potter, B.K.; Davis, T.A.; Bechtold, J.E.; Forsberg, J.A.; et al. Orthopaedic osseointegration: Implantology and future directions. *J. Orthopaed. Res.* **2020**, *38*, 1445–1454. [CrossRef] [PubMed]
2. Verma, A.; Singh, S.V.; Arya, D.; Shivakumar, S.; Chand, P. Mechanical failures of dental implants and supported prostheses: A systematic review. *J. Oral Biol. Craniofac. Res.* **2023**, *13*, 306–314. [CrossRef] [PubMed]

3. Segal, P.; Makhoul, A.; Eger, M.; Lucchina, A.G.; Winocur, E.; Mijiritsky, E. Preliminary Study to Evaluate Marginal Bone Loss in Cases of 2- and 3-Implant-Supported Fixed Partial Prostheses of the Posterior Mandible. *J. Craniofac. Surg.* **2019**, *30*, 1068–1072. [CrossRef] [PubMed]
4. Hingsammer, L.; Pommer, B.; Hunger, S.; Stehrer, R.; Watzek, G.; Insua, A. Influence of Implant Length and Associated Parameters Upon Biomechanical Forces in Finite Element Analyses: A Systematic Review. *Implant Dent.* **2019**, *28*, 296–305. [CrossRef] [PubMed]
5. Fernandes, G.V.O.; Ferreira, N.D.R.N.; Heboyan, A.; Nassani, L.M.; Pereira, R.M.A.; Fernandes, J.C.H. Clinical assessment of short (>6 mm and ≤8.5 mm) implants in posterior sites with an average follow-up of 74 Months: A Retrospective Study. *Int. J. Oral Maxillofac. Implant* **2023**, *38*, 915–926. [CrossRef]
6. Cenkoglu, B.G.; Balcioglu, N.B.; Ozdemir, T.; Mijiritsky, E. The Effect of the Length and Distribution of Implants for Fixed Prosthetic Reconstructions in the Atrophic Posterior Maxilla: A Finite Element Analysis. *Materials* **2019**, *12*, 2556. [CrossRef]
7. Fernandes, G.; Costa, B.; Trindade, H.F.; Castilho, R.M.; Fernandes, J. Comparative analysis between extra-short implants (≤6 mm) and 6 mm-longer implants: A meta-analysis of randomized controlled trial. *Aust. Dent. J.* **2022**, *67*, 194–211. [CrossRef]
8. Markose, J.; Eshwar, S.; Srinivas, S.; Jain, V. Clinical outcomes of ultrashort sloping shoulder implant design: A survival analysis. *Clin. Implant Dent. Relat. Res.* **2018**, *20*, 646–652. [CrossRef]
9. Taschieri, S.; Lolato, A.; Testori, T.; Francetti, L.; Del Fabbro, M. Short dental implants as compared to maxillary sinus augmentation procedure for the rehabilitation of edentulous posterior maxilla: Three-year results of a randomized clinical study. *Clin. Implant Dent. Relat. Res.* **2018**, *20*, 9–20. [CrossRef]
10. Cruz, R.S.; Lemos, C.A.A.; Batista, V.E.S.; Oliveira, H.F.F.E.; Gomes, J.M.L.; Pellizzer, E.P.; Verri, F.R. Short implants versus longer implants with maxillary sinus lift. A systematic review and meta-analysis. *Braz. Oral Res.* **2018**, *32*, e86. [CrossRef]
11. Linetskiy, I.; Demenko, V.; Yefremov, O.; Linetska, L.; Kondratiev, A. Crestal versus subcrestal short plateau implant placement. In *Integrated Computer Technologies in Mechanical Engineering*; ICTM 2023 Lecture Notes in Networks and Systems; Springer International Publishing: Cham, Switzerland, 2024; Volume 1008, pp. 258–267. [CrossRef]
12. Alqahtani, A.R.; Desai, S.R.; Patel, J.R.; Alqhtani, N.R.; Alqahtani, A.S.; Heboyan, A.; Fernandes, G.V.O.; Mustafa, M.; Karobari, M.I. Investigating the impact of diameters and thread designs on the Biomechanics of short implants placed in D4 bone: A 3D finite element analysis. *BMC. Oral Health* **2023**, *23*, 686. [CrossRef] [PubMed]
13. Linetska, L.; Kipenskyi, A.; Demenko, V.; Linetskiy, I.; Kondratiev, A.; Yefremov, O. Finite element study of biomechanical behavior of short dental implants with bone loss effects–evaluation of bone turnover. In Proceedings of the 2023 IEEE 4th KhPI Week on Advanced Technology (KhPIWeek), Kharkiv, Ukraine, 2–6 October 2023; pp. 1–6. [CrossRef]
14. Calì, M.; Zanetti, E.M.; Oliveri, S.M.; Asero, R.; Ciaramella, S.; Martorelli, M.; Bignardi, C. Influence of thread shape and inclination on the biomechanical behaviour of plateau implant systems. *Dent. Mater.* **2018**, *34*, 460–469. [CrossRef] [PubMed]
15. McKenna, G.J.; Gjengedal, H.; Harkin, J.; Holland, N.; Moore, C.; Srinivasan, M. Effect of autogenous bone graft site on dental implant survival and donor site complications: A systematic review and meta-analysis. *J. Evid. Based Dent. Pract.* **2022**, *22*, 101731. [CrossRef] [PubMed]
16. Qiu, P.; Cao, R.; Li, Z.; Fan, Z. A comprehensive biomechanical evaluation of length and diameter of dental implants using finite element analyses: A systematic review. *Heliyon* **2024**, *10*, e26876. [CrossRef] [PubMed]
17. Leucht, P.; Monica, S.D.; Temiyasathit, S.; Lenton, K.; Manu, A.; Longaker, M.T.; Jacobs, C.R.; Spilker, R.L.; Guo, H.; Brunski, J.B.; et al. Primary cilia act as mechanosensors during bone healing around an implant. *Med. Eng. Phys.* **2013**, *35*, 392–402. [CrossRef]
18. Frost, H.M. A 2003 update of bone physiology and Wolff's Law for clinicians. *Angle Orthod.* **2004**, *74*, 3–15. [CrossRef]
19. Frost, H.M. Bone "mass" and the "mechanostat": A proposal. *Anat. Rec.* **1987**, *219*, 1–9. [CrossRef]
20. Misch, C.E. (Ed.) Chapter 32—Progressive Bone Loading: Increasing the Density of Bone with a Prosthetic Protocol. In *Dental Implant Prosthetics*; Mosby: Maryland Heights, MO, USA, 2015; pp. 913–937. [CrossRef]
21. Saab, X.E.; Griggs, J.A.; Powers, J.M.; Engelmeier, R.L. Effect of abutment angulation on the strain on the bone around an implant in the anterior maxilla: A finite element study. *J. Prosthet. Dent.* **2007**, *97*, 85–92. [CrossRef]
22. Falcinelli, C.; Valente, F.; Vasta, M.; Traini, T. Finite element analysis in implant dentistry: State of the art and future directions. *Dent. Mater.* **2023**, *39*, 539–556. [CrossRef]
23. Lisiak-Myszke, M.; Marciniak, D.; Bieliński, M.; Sobczak, H.; Garbacewicz, Ł.; Drogoszewska, B. Application of Finite Element Analysis in Oral and Maxillofacial Surgery-A Literature Review. *Materials* **2020**, *13*, 3063. [CrossRef]
24. Linetskiy, I.; Sutcliffe, M.; Kondratiev, A.; Demenko, V.; Linetska, L.; Yefremov, O. A novel method of load bearing ability analysis of short plateau implants placed in compromised bone. In Proceedings of the 2023 IEEE 4th KhPI Week on Advanced Technology (KhPIWeek), Kharkiv, Ukraine, 2–6 October 2023; pp. 1–6. [CrossRef]
25. Sugiura, T.; Yamamoto, K.; Horita, S.; Murakami, K.; Tsutsumi, S.; Kirita, T. The effects of bone density and crestal cortical bone thickness on micromotion and peri-implant bone strain distribution in an immediately loaded implant: A nonlinear finite element analysis. *J. Periodontal Implant Sci.* **2016**, *46*, 152–165. [CrossRef] [PubMed]
26. Bozkaya, D.; Muftu, S.; Muftu, A. Evaluation of load transfer characteristics of five different implants in compact bone at different load levels by finite elements analysis. *J. Prosthet. Dent.* **2004**, *92*, 523–530. [CrossRef] [PubMed]
27. Lemos, C.A.A.; Verri, F.R.; Noritomi, P.Y.; Kemmoku, D.T.; Souza Batista, V.E.; Cruz, R.S.; de Luna Gomes, J.M.; Pellizzer, E.P. Effect of bone quality and bone loss level around internal and external connection implants: A finite element analysis study. *J. Prosthet. Dent.* **2021**, *125*, 137.e1–137.e10. [CrossRef]

28. Mericske-Stern, R.; Zarb, G.A. In vivo measurements of some functional aspects with mandibular fixed prostheses supported by implants. *Clin. Oral Implants Res.* **1996**, *7*, 153–161. [CrossRef] [PubMed]
29. Sahin, S.; Cehreli, M.C.; Yalçin, E. The influence of functional forces on the biomechanics of implant-supported prostheses—A review. *J. Dent.* **2002**, *30*, 271–282. [CrossRef]
30. Li, J.; Jansen, J.A.; Walboomers, X.F.; van den Beucken, J.J. Mechanical aspects of dental implants and osseointegration: A narrative review. *J. Mech. Behav. Biomed. Mater.* **2020**, *103*, 103574. [CrossRef]
31. Gere, J.M.; Timoshenko, S.P. *Mechanics of Materials*; Chapman & Hall: London, UK, 1991.
32. Kondratiev, A.; Potapov, O.; Tsaritsynskyi, A.; Nabokina, T. Optimal design of composite shelled sandwich structures with a honeycomb filler. In *Advances in Design, Simulation and Manufacturing IV. DSMIE 2021*; Lecture Notes in Mechanical Engineering; Springer: Berlin/Heidelberg, Germany, 2021; pp. 546–555. [CrossRef]
33. Jafarian, M.; Mirhashemi, F.S.; Emadi, N. Finite element analysis of stress distribution around a dental implant with different amounts of bone loss: An in vitro study. *Dent. Med. Probl.* **2019**, *56*, 27–32. [CrossRef]
34. Yalçın, M.; Kaya, B.; Laçin, N.; Arı, E. Three-Dimensional Finite Element Analysis of the Effect of Endosteal Implants with Different Macro Designs on Stress Distribution in Different Bone Qualities. *Int. J. Oral Maxillofac. Implant* **2019**, *34*, e43–e50. [CrossRef]
35. Oliveira, H.; Brizuela Velasco, A.; Ríos-Santos, J.V.; Sánchez, L.F.; Lemos, B.F.; Gil, F.J.; Carvalho, A.; Herrero-Climent, M. Effect of Different Implant Designs on Strain and Stress Distribution under Non-Axial Loading: A Three-Dimensional Finite Element Analysis. *Int. J. Environ. Res. Public Health* **2020**, *17*, 4738. [CrossRef]
36. Chen, J.; Guo, J.; Yang, L.; Wang, L.; Zhang, X. Effect of different implant angulations on the biomechanical performance of prosthetic screws in two implant-supported, screw-retained prostheses: A numerical and experimental study. *J. Prosthet. Dent.* **2023**, *130*, 240.e1–240.e10. [CrossRef]
37. Demenko, V.; Linetskiy, I.; Nesvit, K.; Hubalkova, H.; Nesvit, V.; Shevchenko, A. Importance of diameter-to-length ratio in selecting dental implants: A methodological finite element study. *Comput. Methods Biomech. Biomed. Eng.* **2014**, *17*, 443–449. [CrossRef] [PubMed]
38. Yoda, N.; Zheng, K.; Chen, J.; Li, W.; Swain, M.; Sasaki, K.; Li, Q. Bone morphological effects on post-implantation remodeling of maxillary anterior buccal bone: A clinical and biomechanical study. *J. Prosthodont. Res.* **2017**, *61*, 393–402. [CrossRef] [PubMed]
39. De Matos, J.D.M.; Queiroz, D.A.; Nakano, L.J.N.; Andrade, V.C.; Ribeiro, N.D.R.; Borges, A.L.S.; Bottino, M.A.; Lopes, G.D.S. Bioengineering tools applied to dentistry: Validation methods for in vitro and in silico analysis. *Dent. J.* **2022**, *10*, 145. [CrossRef] [PubMed]
40. Hannam, A.G. Current computational modelling trends in craniomandibular biomechanics and their clinical implications. *J. Oral Rehabil.* **2011**, *38*, 217–234. [CrossRef]
41. Anderson, A.E.; Ellis, B.J.; Weiss, J.A. Verification, validation and sensitivity studies in computational biomechanics. *Comput. Methods Biomech. Biomed. Eng.* **2007**, *10*, 171–184. [CrossRef]
42. Yan, X.; Zhang, X.; Chi, W.; Ai, H.; Wu, L. Comparing the influence of crestal cortical bone and sinus floor cortical bone in posterior maxilla bi-cortical dental implantation: A three-dimensional finite element analysis. *Acta Odontol. Scand.* **2015**, *73*, 312–320. [CrossRef]
43. Okumura, N.; Stegaroiu, R.; Kitamura, E.; Kurokawa, K.; Nomura, S. Influence of maxillary cortical bone thickness, implant design and implant diameter on stress around implants: A three-dimensional finite element analysis. *J. Prosthodont. Res.* **2010**, *54*, 133–142. [CrossRef]
44. Barbosa, F.T.; Zanatta, L.C.S.; de Souza Rendohl, E.; Gehrke, S.A. Comparative analysis of stress distribution in one-piece and two-piece implants with narrow and extra-narrow diameters: A finite element study. *PLoS ONE* **2021**, *16*, e0245800. [CrossRef]
45. Chou, I.-C.; Lee, S.-Y.; Ming-Chang, W.; Sun, C.W.; Jiang, C.P. Finite element modelling of implant designs and cortical bone thickness on stress distribution in maxillary type IV bone. *Comput. Methods Biomech. Biomed. Eng.* **2014**, *17*, 516–526. [CrossRef]
46. Alper, B.; Gultekin, P.; Yalci, S. Application of Finite Element Analysis in Implant Dentistry. In *Finite Element Analysis-New Trends and Developments*; InTech: Rijeka, Croatia, 2012. [CrossRef]
47. Tretto, P.H.W.; Dos Santos, M.B.F.; Spazzin, A.O.; Pereira, G.K.R.; Bacchi, A. Assessment of stress/strain in dental implants and abutments of alternative materials compared to conventional titanium alloy-3D non-linear finite element analysis. *Comput. Methods Biomech. Biomed. Eng.* **2020**, *23*, 372–383. [CrossRef]
48. Limbert, G.; van Lierde, C.; Muraru, O.L.; Walboomers, X.F.; Frank, M.; Hansson, S.; Middleton, J.; Jaecques, S. Trabecular bone strains around a dental implant and associated micromotions--a micro-CT-based three-dimensional finite element study. *J. Biomech.* **2010**, *43*, 1251–1261. [CrossRef] [PubMed]
49. Frost, H.M. The mechanostat: A proposed pathogenic mechanism of osteoporoses and the bone mass effects of mechanical and nonmechanical agents. *Bone. Miner.* **1987**, *2*, 73–85. [PubMed]
50. Grauer, D.; Cevidanes, L.S.; Proffit, W.R. Working with DICOM craniofacial images. *Am. J. Orthod. Dentofac. Orthop.* **2009**, *136*, 460–470. [CrossRef] [PubMed]
51. Bordin, D.; Castro, M.B.; Carvalho, M.A.; Araujo, A.M.; Cury, A.A.D.B.; Lazari-Carvalho, P.C. Different Treatment Modalities Using Dental Implants in the Posterior Maxilla: A Finite Element Analysis. *Braz. Dent. J.* **2021**, *32*, 34–41. [CrossRef] [PubMed]

52. Khosravani, M.R. Mechanical behavior of restorative dental composites under various loading conditions. *J. Mech. Behav. Biomed. Mater.* **2019**, *93*, 151–157. [CrossRef]
53. Kurniawan, D.; Nor, F.M.; Lee, H.Y.; Lim, J.Y. Finite element analysis of bone-implant biomechanics: Refinement through featuring various osseointegration conditions. *Int. J. Oral Maxillofac. Surg.* **2012**, *41*, 1090–1096. [CrossRef]